





Sprayed water microdroplets containing dissolved pyridine spontaneously generate pyridyl anions

Lingling Zhao^a, Xiaowei Song^b, Chu Gong^a, Dongmei Zhang^a, Ruijing Wang^a, Richard N. Zare^{b,1} , and Xinxing Zhang^{a,1} 

Contributed by Richard Zare; received January 18, 2022; accepted February 8, 2022; reviewed by Joseph Francisco and Kenneth Jordan

The anion of pyridine, $C_5H_5N^-$, has been thought to be short lived in the gas phase and was only previously observed indirectly. In the condensed phase, $C_5H_5N^-$ is known to be stabilized by solvation with other molecules. We provide in this study striking results for the formation of isolated $C_5H_5N^-$ from microdroplets of water containing dissolved pyridine observed in the negative ion mass spectrum. The gas-phase lifetime of $C_5H_5N^-$ is estimated to be at least 50 ms, which is much longer than previously thought. The generated $C_5H_5N^-$ captured CO_2 molecules to form a stable $(Py-CO_2)^-$ complex, further confirming the existence of $C_5H_5N^-$. We propose that the high electric field at the air–water interface of a microdroplet helps OH^- to transfer an electron to pyridine to form $C_5H_5N^-$ and the hydroxyl radical $\bullet OH$. Oxidation products of the Py reacting with $\bullet OH$ are also observed in the mass spectrum recorded in positive mode, which further supports this mechanism. The present study pushes the limits of the reducing and oxidizing power of water microdroplets to a new level, emphasizing how different the behavior of microdroplets can be from bulk water. We also note that the easy formation of $C_5H_5N^-$ in water microdroplets presents a green chemistry way to synthesize value-added chemicals.

microdroplet | pyridine | negative ion | air–water interface | hydroxyl

The benzene molecule (C_6H_6) is centrally important to chemistry. The pyridine molecule (C_5H_5N ; which we will denote by Py) is structurally related to benzene with one methine group ($=CH^-$) replaced by a nitrogen atom in the six-membered ring. The isolated benzene molecule does not form a stable negative ion ($C_6H_6^-$) in the gas phase. Similarly, pyridine has been thought not to form a stable negative ion ($C_5H_5N^-$), which is called the pyridyl anion. Imagine then our surprise to discover that when room-temperature water containing dissolved pyridine is sprayed to form tiny water droplets, we detected the pyridyl anion using a mass spectrometer operated in negative ion mode. This observation is made with no external voltage applied to microdroplets sprayed from a fused-silica capillary with N_2 gas flow coaxial to the capillary. The measured mass-to-charge ratio clearly identifies that we are observing the $C_5H_5N^-$ anion. In what follows, we call $C_5H_5N^-$ the pyridyl anion, Py^- , but we do not know its structure, and we cannot rule out the possibility that it is some isomer of Py that forms a negative ion, although we suspect it is not that.

There has been much work pointing to the existence of unstable negative ions of polyatomic molecules, and an excellent review has been provided by Jordan and Burrow (1). In the case of $C_5H_5N^-$, the isolated anion has only been detected indirectly using the SF_6 -scavenger method (2), using the electron trapping method (3, 4), and by recording the derivative of the total electron-scattering cross section as a function of energy when a monoenergetic beam of electrons is transmitted through pyridine vapor (5–8). A so-called shape resonance occurs around 0.6 to 0.7 eV (5, 8), indicating a temporarily bound negative ion of pyridine in the gas phase. This conclusion is further supported by theoretical calculations (9, 10). The failure to observe $C_5H_5N^-$ (which we denote by Py^-) in the gas phase has been attributed by Compton and coworkers (2) to the unstable anion's short lifetime which was estimated to be less than a microsecond.

The isolated pyridine anion $C_5H_5N^-$ is thought to be unstable, whereas in an aqueous solution, it is known to be stabilized by clustering with water. The first experimental evidence for this behavior was provided by Desfrancois and coworkers (11) who prepared water clusters of different sizes by a supersonic expansion of a pyridine:water solution in which electron transfer occurs from a Rydberg-excited atom to form the negative ion cluster. It was reported that the cluster size threshold was $n = 3$ to stabilize the $C_5H_5N^-$, i.e., $[C_5H_5N\bullet(H_2O)_n]^-$ only forms for $n \geq 3$. This finding has been subsequently confirmed by work of Johnson and coworkers (12) who attributed the stabilization of $C_5H_5N^-$ by the water cluster to two effects as follows: 1) the dielectric constant

Significance

Water microdroplets can accelerate chemical reactions by orders of magnitude compared to the same reactions in bulk water and/or trigger spontaneous reactions that do not occur in bulk solution. Among the properties of water microdroplets, the unique redox ability resulting from the spontaneous dissociation of OH^- into a released electron and $\bullet OH$ at the air–water interfaces is especially intriguing. At the air–water interface, OH^- exhibits a strong reducing potential, and the resulting $\bullet OH$ is highly oxidative, making water microdroplets a unity of opposites. We report the reduction of pyridine into pyridyl anions ($C_5H_5N^-$) and the oxidation of pyridine into hydroxypyridine, which extends what we know about the redox power of water microdroplets.

Author affiliations: ^aCollege of Chemistry, Key Laboratory of Advanced Energy Materials Chemistry (Ministry of Education), Renewable Energy Conversion and Storage Center (ReCAST), Beijing National Laboratory for Molecular Sciences, Shenzhen Research Institute, Frontiers Science Center for New Organic Matter, Nankai University, Tianjin 300071, China; and ^bDepartment of Chemistry, Stanford University, Stanford, CA 94305

Author contributions: R.N.Z. and X.Z. designed research; L.Z., X.S., C.G., D.Z., and R.W. performed research; L.Z., X.S., R.N.Z., and X.Z. analyzed data; and L.Z., X.S., R.N.Z., and X.Z. wrote the paper.

Reviewers: J.F., University of Pennsylvania; and K.J., University of Pittsburgh.

The authors declare no competing interest.

Copyright © 2022 the Author(s). Published by PNAS. This article is distributed under [Creative Commons Attribution-NonCommercial-NoDerivatives License 4.0 \(CC BY-NC-ND\)](https://creativecommons.org/licenses/by-nc-nd/4.0/).

See [online](https://www.pnas.org/lookup/suppl/doi:10.1073/pnas.2200991119/-/DCSupplemental) for related content such as Commentaries.

¹To whom correspondence may be addressed. Email: rnz@stanford.edu or zhangxx@nankai.edu.cn.

This article contains supporting information online at [http://www.pnas.org/lookup/suppl/doi:10.1073/pnas.2200991119/-/DCSupplemental](https://www.pnas.org/lookup/suppl/doi:10.1073/pnas.2200991119/-/DCSupplemental).

Published March 14, 2022.

of water that helps to prevent electron autodetachment and 2) proton transfer that stabilizes the nascent hydroxide anion. Combining the results from photoelectron spectroscopy with computational chemistry suggests that the $[\text{C}_5\text{H}_5\text{N}\bullet(\text{H}_2\text{O})_n \geq 3]^-$ cluster is best described as a combination of hydrated $\text{C}_5\text{H}_5\text{N}^-$ and the neutral pyridinyl radical PyH formed by electron-induced proton transfer for $n = 3$ but as $\text{PyH}\bullet(\text{OH}^-)\bullet(\text{H}_2\text{O})_{n-1}$ for $n \geq 4$ (13). The pyridyl anion has been produced in the condensed phase in many different ways, and it has also been extensively spectroscopically studied (14–26).

In recent years, many studies have shown that chemical reactions in water microdroplets behave markedly differently from the same reaction conditions in bulk water solutions, such as causing remarkable acceleration of reaction rates (27, 28). Another special property of aqueous microdroplet chemistry is the production of reaction products that differ markedly from those found in bulk solution reactions. Examples are the reduction of chloroauric acid (HAuCl_4) to gold nanoparticles (29), the reduction of a number of different carboxylic acids (30), and the formation of hydrogen peroxide (31, 32). The reasons for this behavior are not fully established but point to chemistry occurring at the air–water interface (AWI), whose importance in aerosol chemistry has been emphasized by Francisco and coworkers (33). The present study concerns the reduction of pyridine in water microdroplets which allows the direct observation of the pyridine anion in the gas phase.

Results and Discussion

Spontaneous Generation of $\text{C}_5\text{H}_5\text{N}^-$ in Water Microdroplets.

The experimental setup is shown in Fig. 1A. A pyridine:water solution is prepared and forced by a syringe pump through a capillary that sits inside a larger capillary through which N_2 gas flows at high pressure. The resulting spray of microdroplets is aimed toward the heated inlet of a mass spectrometer operated in negative ion mode. Fig. 1B presents a typical mass spectrum showing

the spontaneous generation of Py^- at m/z 79 when the pyridine:water solution is sprayed to form microdroplets. Pure water shows no peaks over the mass range covered in this figure. Detailed experimental conditions are described in *Materials and Methods*. Because the observation of the pyridyl anion was unexpected, spray experiments were repeated separately at both Nankai University and Stanford University. Fig. 1C illustrates how the Py^- intensity depends on the pyridine concentration in water. The mass spectrum of each different pyridine:water solution was recorded for a duration of at least 1 min. This information allowed us to determine how the efficiency of Py^- generation varies with Py concentration, as presented in Fig. 1C. Fig. 1D shows the relative efficiency of Py^- generation from different solutions, where the error bars are estimated from the intensity fluctuations in Fig. 1C, and the efficiency of the 100 mM pyridine solution is set as 1. The observation that a lower concentration yields a much higher Py^- generation efficiency suggests that the AWI of the water microdroplets plays a key role in the reactions because lower concentrations cause higher fractions of the solute molecules to partition into the AWI of microdroplets (30, 34). To further investigate the significance of the AWI of the microdroplets, we also monitored the Py^- intensity when the sheath gas pressure was changed (Fig. 1E). A clear increase in the intensity of Py^- was observed upon consecutively increasing the pressure from 80 psi to 120 psi and then to 160 psi. It is known that increasing the pressure decreases the sizes and increases the ratios of surface area to volume of the microdroplets (35), which again demonstrates the importance of the microdroplet AWI. We also examined the temperature dependence (Fig. 1F). The intensity of Py^- first increases when the inlet temperature of the mass spectrometer increases from 70 °C to 170 °C but falls off in going from 170 °C to 275 °C. The lack of monotonicity might be a result of two competing effects, namely, the heating of the system accelerates the reduction but at a higher temperature the decay of Py^- becomes dominant. To avoid the possibility that pyridine reduction might be triggered by trace

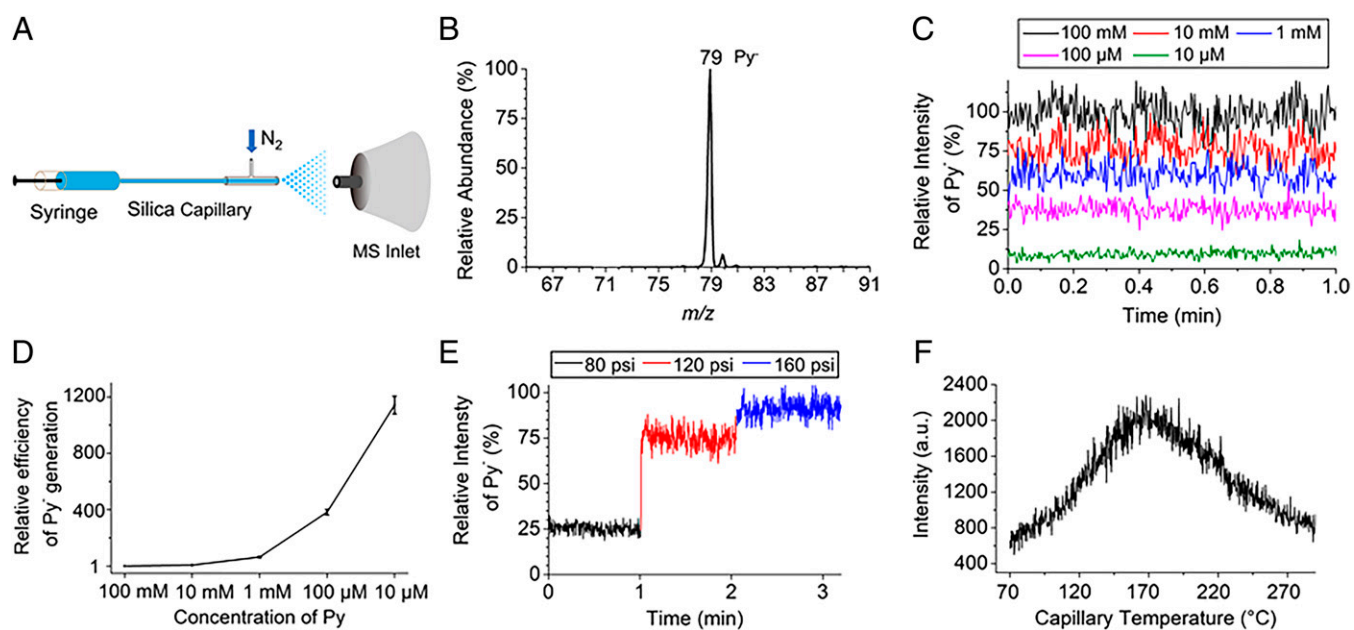


Fig. 1. Mass spectrometric analyses of the spontaneous generation of $\text{C}_5\text{H}_5\text{N}^-$ in water microdroplets. (A) Schematic drawing of the experimental setup. (B) Typical mass spectrum showing the Py^- anion when the concentration of Py is 100 μM . (C) Relative intensities of Py^- when the concentrations of Py solutions are 100 mM, 10 mM, 1 mM, 100 μM , and 10 μM . (D) The relative efficiency for Py^- generation as a function of Py concentration calculated from the data in C. The efficiency of the 100 mM solution is set as 1, and each error bar is estimated from the intensity fluctuations in C. (E) Relative intensities of Py^- when the sheath gas pressure is increased stepwise from 80 to 120 and then to 160 psi. (F) The change of Py^- intensity when the mass spectrometer inlet capillary temperature is gradually increased from 70 to 275 °C.

species in the atmosphere, we also performed the experiment with a mass spectrometer whose inlet is inserted into a pure N_2 -protected glove box (36). No difference in Py^- signal intensity was observed (*SI Appendix, Fig. S1*).

Capture of $C_5H_5N^-$ with CO_2 . In 2000, Kim and coworkers (37) made a stable planar C_{2v} anionic complex $(Py-CO_2)^-$ by the electron attachment to CO_2 and Py (Fig. 2A for the structure). The complex was characterized by anion photoelectron spectroscopy, which revealed a high vertical detachment energy of 1.46 eV. Calculations showed a π -conjugated network throughout the whole molecule. Both CO_2 and Py have negative electron affinities so that the fact that the anionic complex can form might be thought to be initially surprising. An explanation is that the extended π -conjugated system over the entire complex allows the accommodation of the extra electron. Moreover, CO_2 behaves as a Lewis acid (in general) so that it is expected to like electron-rich systems, while Py is a Bronsted base. Later, Johnson and coworkers (38) studied the same system using infrared photodissociation techniques. Motivated by these previous studies, we performed the microdroplet experiment using CO_2 in place of N_2 as the sheath gas for the purpose of capturing the $C_5H_5N^-$ anion in the form of the $(Py-CO_2)^-$ complex. Fig. 2B presents the mass spectra with either N_2 or CO_2 as the sheath gas. A prominent new peak at m/z 123 corresponding to the $(Py-CO_2)^-$ product shows up when using CO_2 . This experiment was also performed in the glove box, and no difference was observed (*SI Appendix, Fig. S2*).

To understand better the reaction pathway, we performed density functional theory (DFT) calculations for the system at the $\omega B97XD/aug-cc-pVDZ$ level of theory. Fig. 2A plots the potential energy surface for the $(Py-CO_2)^-$ system as a function of the N-C bond length with the remainder of the complex relaxed to its ground state. There is only one potential well along the N-C coordinate, meaning that this is a barrier-free reaction. The well corresponds to the fully optimized structure with a N-C bond length of 1.50 Å. The highest singly occupied molecular orbital (HOMO) of the optimized structure shows delocalized π conjugation over the whole molecule, explaining its stability. To confirm that the reaction indeed occurs between anionic Py^- and neutral CO_2 but not between neutral Py and anionic CO_2^- , the HOMO of the structure with the CO_2 and Py moieties separated by 4.0 Å shows that the electron density solely occupies the π^* antibonding orbital of Py. In addition, natural population analysis (NPA), as implemented in the Gaussian 09 code, was also carried out to determine the charge distributions. In the fully optimized structure, the CO_2 and Py moieties are negatively charged by -0.34 and $-0.66 e$, respectively, again confirming the electron delocalization. But,

in the structure where the CO_2 and Py moieties are separated by 4.0 Å, the entire $-1.00 e$ charge is on the Py ring. Taken together, the reaction occurs between anionic $C_5H_5N^-$ and neutral CO_2 in a barrier-free manner.

Estimation of the Lifetime of Py^- . The lower bound on the lifetime of gas-phase $C_5H_5N^-$ can be roughly estimated using the collision-induced dissociation (CID) mode of the LTQ-XL mass spectrometer. We find that the Py^- signal disappears even though the collision energy is set to be 0 eV (*SI Appendix, Fig. S3*). A full scan of a mass spectrum in LTQ-XL takes ~ 50 ms (39). However, in the CID mode, the mass spectrometer needs a much longer ion injection time and extra ion isolation and activation time that is not required for the full scan mode. As a result, a CID cycle takes ~ 250 ms (39). The disappearance of the m/z 79 peak during CID might be a result of the autodeachment of the unstable $C_5H_5N^-$ anion or its collisional breakup. Hence, we estimate that the gas-phase lifetime of Py^- must be greater than 50 ms, which is many orders of magnitude longer than what was first expected (2, 5). We cannot rule out the possibility that gas-phase $C_5H_5N^-$ is a stable anion but highly fragile. When we used an orbitrap (Velos Pro, Thermo Fisher, Waltham, MA) high-resolution mass spectrometer to record the pyridine:water microdroplet mass spectrum, we failed to find the expected mass peak of Py^- at 79.0416. Again, this observation appears to be consistent with the disappearance of this negative ion for long observation times.

For molecules with negative electron affinities, autodeachment lifetimes of their negative ions are typically less than a picosecond. However, closed-shell molecules with large dipole moments can bind an extra electron, and it has been suggested by Crawford (40) in 1971 that any real gas-phase molecule or radical with a dipole moment greater than 2.0 Debye probably can bind an electron and almost certainly can if the dipole moment is greater than 2.5 Debye. Pyridine has a dipole moment of about 2.2 Debye (41), making it borderline. It remains to be determined whether $C_5H_5N^-$, which we are denoting by Py^- , is best described as a nonvalence correlation-bound anion (42). We know for sure that we are observing in the gas phase $C_5H_5N^-$, which we call the pyridyl anion, but, as stated before, we do not know its structure.

Mechanism of $C_5H_5N^-$ Generation in Microdroplets. The detailed mechanism for the formation of Py^- in water microdroplets remains to be established, but the following represents what we think might be some important clues. First, water is necessary for $C_5H_5N^-$ formation. When microdroplets of pure Py are sprayed, no $C_5H_5N^-$ is observed. Second, when a benzene:water mixture is sprayed, no benzene negative ion is

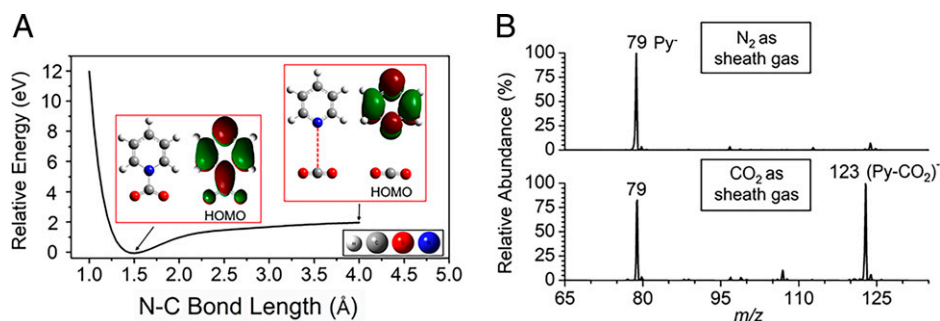


Fig. 2. The capture of Py^- with CO_2 . (A) DFT calculation results of the potential energy surface along the N-C bond of the $(Py-CO_2)^-$ system at the $\omega B97XD/aug-cc-pVDZ$ level of theory. Typical structures and their corresponding HOMOs along the scanned coordinate are also displayed. (B) Typical mass spectra using N_2 (Top) or CO_2 (Bottom) as the sheath gas.

observed. Pyridine differs from benzene in that Py readily forms PyH^+ in water, whereas benzene is not protonated by water. Thus, we expect that the reaction might involve PyH^+ and water at the AWI, although we cannot exclude the possibility that it is just Py and water at the AWI.

A major question is where does the electron come from that is captured by pyridine? One possibility would be from HCO_3^- arising from trace amounts of dissolved CO_2 . However, the addition of calcium chloride to the solution reduces the concentration of HCO_3^- but does not fully eliminate its presence, whereas the $\text{C}_5\text{H}_5\text{N}^-$ signal is not strongly affected, suggesting that dissolved CO_2 is not the major source. It seems then that the most plausible answer is from OH^- at the AWI. The standard reduction potential of $\bullet\text{OH}/\text{OH}^-$ appears to lie between 2.10 V at pH = 0 and 1.25 V at pH = 14 (43). If we assume that this potential acts over 5×10^{-8} cm, this corresponds to an electric field of 2×10^7 to 4×10^7 V/cm. Recently, Head-Gordon and coworkers (44) calculated that the electric field alignments along free O–H bonds at the AWI are $\sim 1.6 \times 10^7$ V/cm larger on average than that found for O–H bonds in the interior of the water droplet. This estimate is in good agreement with the measured electric field strength of a water microdroplet in oil (45). It seems then that the electric field at the AWI is sufficiently strong that it can assist OH^- to release its electron. It also seems likely that the reduction potential of $\bullet\text{OH}/\text{OH}^-$ is lowered in value caused by OH^- crowding at the AWI (46). We speculate that PyH^+ recombines with OH^- to yield Py and H_2O liberating energy that may help the newly formed Py to capture an electron from OH^- at the AWI to form $\text{Py}^- + \bullet\text{OH}$. It is also possible that OH^- directly transfers an electron to Py at the AWI, again to form $\text{Py}^- + \bullet\text{OH}$.

Some support for these speculations is shown in Fig. 3, which is the mass spectrum from sprayed pyridine:water microdroplets recorded in positive ion mode. Four major peaks are observed. The most prominent peak at m/z 80 belongs to the pyridinium cation, PyH^+ . The peak at m/z 96 is the product of Py being oxidized by $\bullet\text{OH}$, yielding an *m*-hydroxypyridine molecule in the protonated form. Previous studies revealed that the reaction between Py and $\bullet\text{OH}$ mainly produced *m*-hydroxypyridine but not the *o*- or *p*-isomers, owing to the electron-rich nature of the carbon atom of pyridine in the meta position (47). The peak at m/z 112 is the protonated 3, 5-dihydroxypyridine product from the oxidation of Py by two $\bullet\text{OH}$ radicals. The observation of Py

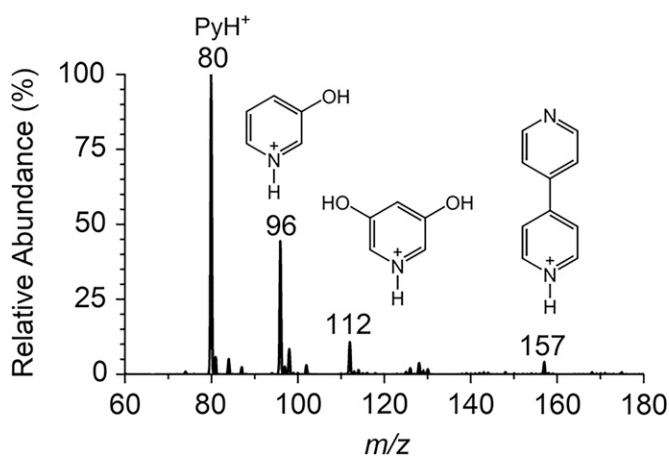


Fig. 3. Positive mode mass spectrum of water microdroplets containing dissolved pyridine. The major mass peaks are protonated pyridine $m/z = 80$, protonated *m*-hydroxypyridine $m/z = 96$, protonated 3,5-dihydroxypyridine $m/z = 112$, and protonated 4,4'-bipyridine $m/z = 157$.

oxidation provides more indirect evidence for the existence of $\bullet\text{OH}$ at the AWI of microdroplets, adding to previous evidence in which salicylic acid was used to successfully scavenge $\bullet\text{OH}$ (31). In solutions of alkali metals in anhydrous pyridine, a reaction between two pyridyl anions was reported to predominantly generate the 4, 4'-bipyridine product (16). The m/z 157 peak in Fig. 3 is the protonated 4,4'-bipyridine ion. This observation again confirms that Py^- is generated from the microdroplet but not in the gas phase during the MS sampling because it is improbable for two anions to collide with each other in the gas phase. We also found that as the travel distance (reaction time) of the microdroplets was increased, more products were formed (*SI Appendix, Fig. S4*) as expected.

Conclusion

The present work has solidly established that the AWI of aqueous microdroplets can spontaneously generate Py^- , a radical anion that was thought to be extremely unstable and short-lived in the gas phase. However, in this study, the gas-phase lifetime of Py^- is estimated to be at least 50 ms in order to survive the full detection cycle of the mass spectrometer. Measurements are made concerning the concentration, pressure, and temperature dependence for the Py^- generation efficiency, which reveals the controlling role that the AWI of the microdroplets plays. The generated Py^- is captured by CO_2 molecules in the form of a stable $(\text{Py}-\text{CO}_2)^-$ complex, and the formation of 4,4'-bipyridine further confirms the existence of Py^- in microdroplets of pyridine dissolved in water. It is thus concluded that the reducing power of the AWI of water microdroplets is comparable to that of an alkali metal. We also note that the potential use of the easily formed Py^- in water microdroplets presents a green chemistry way to synthesize value-added chemicals, which is a topic for future studies.

Materials and Methods

Materials. At Nankai University, pyridine was purchased from Shanghai Titan Scientific Co., Ltd. Ultra-high purity N_2 was purchased from Air Liquide Co., Ltd. CO_2 was purchased from Tianjin BestGas Co., Ltd. Pure water was purchased from Guangzhou Zhencui Quality Inspection Technology Service Co., Ltd. At Stanford University, water (high-performance liquid chromatography grade, lot 215299) and pyridine (99.0%, anhydrous, lot B0537990) were purchased from Thermo-Fisher Scientific. Ultrapure liquified nitrogen (99.998%) was ordered from the Praxair (NI 4.8LC160Z-22N, Linde Nitrogen).

Generation of Microdroplets and Mass Spectrometric Analyses. A schematic drawing of the experimental setup for the microdroplet reactions is provided in Fig. 1A. Water solutions of Py were sprayed to generate microdroplets by using a syringe pump at a $15\text{-}\mu\text{L}/\text{min}$ flow rate with high-purity nitrogen at 80 to 160 psi as the nebulizing gas. The inner diameter of the fused silica capillary used for spraying was $100\text{ }\mu\text{m}$. When the sheath gas was 80 psi, the size of microdroplets generated was $\sim 7\text{ }\mu\text{m}$ (35). Unlike electrospray ionization, no voltage was applied to the solutions. The distance between the tip of the silica capillary and the mass spectrometer inlet was defined as the reaction distance and was kept at 15 mm unless specified. The products were detected and analyzed by an LTO-XL mass spectrometer (Thermo-Fisher). The employed mass spectrometers in this study were the same models at Nankai University and Stanford University. The inlet capillary temperature of the mass spectrometer changed from 70°C to 275°C to study the temperature dependence. The capillary voltage was set at -50 V . The tube lens voltage on the LTO-XL is set to be 0 V for the detection of $\text{C}_5\text{H}_5\text{N}^-$. To capture the $\text{C}_5\text{H}_5\text{N}^-$ anion with CO_2 , the sheath gas was simply changed from N_2 to CO_2 . To avoid the possibility that the reaction might be triggered by the species in the atmosphere, we also performed the $\text{C}_5\text{H}_5\text{N}^-$ generation and capture experiments with a mass spectrometer whose inlet was inserted into a glove box filled with pure N_2 (36). An extended inlet (3 cm) of an LTO-XL mass spectrometer was inserted into a glove box through an Ultra-Torr fitting

welded to the wall of the glove box. Inside the glove box, the spray experiments were performed similarly as those performed in the atmosphere.

Theoretical Methods. Density functional theory calculations are performed with the Gaussian 09 software package to optimize the structures of anionic (Py-CO₂)⁻ and to scan the potential energy surface of the (Py-CO₂)⁻ system at the ωB97XD/aug-cc-pVDZ level of theory. The potential energy surface is scanned along the C-N coordinate with a step width of 0.05 Å by relaxing the rest of the molecule to its ground state, and the scanning range is 1.0 to 4.0 Å. NPA is used to calculate the charge distribution of the (Py-CO₂)⁻ complex with a C-N bond length of 1.5 Å and 4.0 Å, respectively.

1. K. D. Jordan, P. D. Burrow, Temporary anion states of polyatomic hydrocarbons. *Chem. Rev.* **87**, 557-588 (1987).
2. R. H. Huebner, R. N. Compton, H. C. Schweinler, Temporary negative ion resonance of pyridine. *Chem. Phys. Lett.* **2**, 407-408 (1968).
3. H. H. Brongersma, "The interaction of molecules with low-energy (0 to 30 eV) electrons," PhD thesis, Leiden Rijksuniversiteit, Leiden, The Netherlands (1968).
4. M. N. Pisanias, L. G. Christophorou, J. G. Carter, D. L. McCorkle, Compound-negative-ion resonance states and threshold-electron excitation spectra of N-heterocyclic molecules: Pyridine, pyridazine, pyrimidine, pyrazine, and sym-triazine. *J. Chem. Phys.* **58**, 2110-2124 (1973).
5. I. Nenner, G. J. Schulz, Temporary negative ions and electron affinities of benzene and N-heterocyclic molecules: Pyridine, pyridazine, pyrimidine, pyrazine, and s-triazine. *J. Chem. Phys.* **62**, 1747-1758 (1975).
6. D. Mathur, J. B. Hasted, Temporary negative-ion states in pyridine and diazine molecules. *Chem. Phys.* **16**, 347-352 (1976).
7. P. D. Burrow, A. J. Ashe III, D. J. Bellville, K. D. Jordan, Temporary anion states of phosphabenzene, arsabenzene, and stibabenzene. Trends in the π and π^* orbital energies. *J. Am. Chem. Soc.* **104**, 425-429 (1982).
8. A. Modelli, P. D. Burrow, Electron-transmission study of the temporary anion states of substituted pyridines. *J. Electron Spectrosc. Relat. Phenom.* **32**, 263-276 (1983).
9. A. S. Barbosa, D. F. Pastega, M. H. F. Bettega, Shape resonances in the elastic scattering of slow electrons by pyridine. *Phys. Rev. A* **88**, 022705 (2013).
10. A. Sieradzka, et al., Electron scattering from pyrazine. *J. Phys. Chem. A* **118**, 6657-6663 (2014).
11. V. Periquet, A. Moreau, S. Carles, J. P. Schermann, C. Desfrancois, Cluster size effects upon anion solvation of N-heterocyclic molecules and nucleic acid bases. *J. Electron Spectrosc. Relat. Phenom.* **106**, 141-151 (2000).
12. A. F. DeBlase et al., Water network-mediated, electron-induced proton transfer in [C₅H₅N · (H₂O)_n] clusters. *J. Chem. Phys.* **143**, 144305 (2015).
13. Y. Wang et al., The onset of electron-induced proton-transfer in hydrated azabenzene cluster anions. *Phys. Chem. Chem. Phys.* **18**, 704-712 (2016).
14. J. W. Dodd, F. J. Hopton, N. S. Hush, Electronic spectra of azabenzene anions. *Proc. Chem. Soc.* 61-62 (1962).
15. J. Chaudhuri, S. Hume, J. Jagur-Grodzinski, M. Szwarc, Chemistry of radical anions of heterocyclic aromatics. I. Electron spin resonance and electronic spectra. *J. Am. Chem. Soc.* **90**, 6421-6425 (1968).
16. C. D. Schmulbach, C. C. Hinckley, D. Wasmund, Solutions of alkali metals in anhydrous pyridine. *J. Am. Chem. Soc.* **90**, 6600-6602 (1968).
17. A. Grimison, G. A. Simpson, M. Trujillo Sánchez, J. Jhaveri, Electron attachment by pyridine and the diazines in γ radiolysis. Experimental and theoretical consideration. *J. Phys. Chem.* **73**, 4064-4070 (1969).
18. A. R. Buick, T. J. Kemp, G. T. Neal, T. J. Stone, Electron spin resonance studies of reduction by solvated electrons in liquid ammonia. Part II. Pyridines. *J. Chem. Soc. A* **1969**, 1609-1613 (1969).
19. K. B. Wiberg, T. P. Lewis, Polarographic reduction of the azines. *J. Am. Chem. Soc.* **92**, 7154-7160 (1970).
20. V. Kalyanaraman, C. N. R. Rao, M. V. George, Radical anions of pyridine derivatives. *J. Chem. Soc. B* **1971**, 2406-2409 (1971).
21. P. Neta, Electron spin resonance study of radicals produced by one-electron reduction of pyridines. *Radiat. Res.* **52**, 471-480 (1972).
22. R. W. Fessenden, P. Neta, ESR spectra of radicals produced by reduction of pyridine and pyrazine. *Chem. Phys. Lett.* **18**, 14-17 (1973).
23. W. Lubitz, T. Nyrrönen, ¹⁴N and ¹H ENDOR and TRIPLE resonance on azaaromatic radicals produced by sodium reduction in liquid ammonia. *J. Magn. Reson.* **41**, 17-29 (1980).
24. K. Lühder, H. Füllbier, Zur reaktion der alkalimetalle mit pyridin und seinen substituierprodukten. *Z. Chem* **28**, 402-404 (1988).
25. F. Misaizu, K. Mitsuke, T. Kondow, K. Kuchitsu, Formation of negative ions from pyridine clusters in collision with high-Rydberg rare-gas atoms and slow electrons. *J. Phys. Chem.* **93**, 4263-4266 (1989).
26. J. Schröder et al., Isolation of a stable pyridine radical anion. *Chem. Commun. (Camb.)* **55**, 1322-1325 (2019).
27. X. Yan, R. M. Bain, R. G. Cooks, Organic reactions in microdroplets: Reaction acceleration revealed by mass spectrometry. *Angew. Chem. Int. Ed. Engl.* **55**, 12960-12972 (2016).
28. Z. Wei, Y. Li, R. G. Cooks, X. Yan, Accelerated reaction kinetics in microdroplets: Overview and recent developments. *Annu. Rev. Phys. Chem.* **71**, 31-51 (2020).
29. J. K. Lee, D. Samanta, H. G. Nam, R. N. Zare, Spontaneous formation of gold nanostructures in aqueous microdroplets. *Nat. Commun.* **9**, 1562 (2018).
30. J. K. Lee, D. Samanta, H. G. Nam, R. N. Zare, Micrometer-sized water droplets induce spontaneous reduction. *J. Am. Chem. Soc.* **141**, 10585-10589 (2019).
31. J. K. Lee et al., Spontaneous generation of hydrogen peroxide from aqueous microdroplets. *Proc. Natl. Acad. Sci. U.S.A.* **116**, 19294-19298 (2019).
32. J. K. Lee et al., Condensing water vapor to droplets generates hydrogen peroxide. *Proc. Natl. Acad. Sci. U.S.A.* **117**, 30934-30941 (2020).
33. M. T. C. Martins-Costa, J. M. Anglada, J. S. Francisco, M. F. Ruiz-Lopez, Reactivity of atmospherically relevant small radicals at the air-water interface. *Angew. Chem. Int. Ed. Engl.* **51**, 5413-5417 (2012).
34. K. R. Wilson et al., A kinetic description of how interfaces accelerate reactions in micro-compartments. *Chem. Sci. (Camb.)* **11**, 8533-8545 (2020).
35. Y. H. Lai, S. Sathyamoorthi, R. M. Bain, R. N. Zare, Microdroplets accelerate ring opening of epoxides. *J. Am. Soc. Mass Spectrom.* **29**, 1036-1043 (2018).
36. D. Zhang et al., Revisiting the hitherto elusive cyclohexanehexone molecule: Bulk synthesis, mass spectrometry, and theoretical studies. *J. Phys. Chem. Lett.* **12**, 9848-9852 (2021).
37. Y. Han, I. Chu, J. H. Kim, J. K. Song, S. K. Kim, Photoelectron spectroscopy and ab initio study of mixed cluster anions of [(CO₂)₁₋₃(Pyridine)₁₋₂]⁻: Formation of a covalently bonded anion core of (C₅H₅N-CO₂). *J. Chem. Phys.* **113**, 596-601 (2000).
38. M. Z. Kamrath, R. A. Relph, M. A. Johnson, Vibrational predissociation spectrum of the carbamate radical anion, C₅H₅N-CO₂⁻, generated by reaction of pyridine with (CO₂)_(m)⁻. *J. Am. Chem. Soc.* **132**, 15508-15511 (2010).
39. T. P. Second et al., Dual-pressure linear ion trap mass spectrometer improving the analysis of complex protein mixtures. *Anal. Chem.* **81**, 7757-7765 (2009).
40. O. H. Crawford, Negative ions of polar molecules. *Mol. Phys.* **20**, 585-591 (1971).
41. A. D. Buckingham et al., The dipole moments of pyridine, quinoline, and isoquinoline as vapours and as solutes. *J. Chem. Soc.* **1956**, 1405-1411 (1956).
42. V. K. Voora, A. Kairalapova, T. Sommerfeld, K. D. Jordan, Theoretical approaches for treating non-valence correlation-bound anions. *J. Chem. Phys.* **147**, 214114 (2017).
43. G. Stein, Standard electrode potential of the OH⁻ ion. Correlation with absorption spectrum and energy of solvation. *J. Chem. Phys.* **42**, 2986 (1965).
44. H. Hao, I. Leven, T. Head-Gordon, Can electric fields drive chemistry for an aqueous microdroplet? *Nat. Commun.* **13**, 280 (2022).
45. H. Xiong, J. K. Lee, R. N. Zare, W. Min, Strong electric field observed at the interface of aqueous microdroplets. *J. Phys. Chem. Lett.* **11**, 7423-7428 (2020).
46. Y. B. Vogel et al., The corona of a surface bubble promotes electrochemical reactions. *Nat. Commun.* **11**, 6323 (2020).
47. N. Selvarajan, N. V. Raghavan, Reaction of OH with pyridine. Pulse-radiolytic and product-analysis studies. *J. Phys. Chem.* **84**, 2548-2551 (1980).

Data Availability. All study data are included in the article and/or *SI Appendix*.

ACKNOWLEDGMENTS. X.Z. acknowledges the National Natural Science Foundation of China (NSF) (22003027 and 22174073), the National Key Research and Development (R&D) Program of China (2018YFE0115000), the NSF of Tianjin City (21JCJQJC00010), the Beijing National Laboratory for Molecular Sciences (BNLMS202106), and the Frontiers Science Center for New Organic Matter at Nankai University (63181206). R.N.Z. acknowledges support from the Air Force Office of Scientific Research through the Basic Research Initiative (AFOSR FA9550-16-1-0113) and the Multidisciplinary University Research Initiative (MURI) program (AFOSR FA9550-21-1-0170).